4 WD Urban Electric Vehicle Motion Studies Based on MIMO Fuzzy Logic Speed Controller

Brahim Gasbaoui, Abdelfatah Nasri, Abdellah Laoufi and Youssef Mouloudi
Faculty of the sciences and technology, Bechar University
B.P 417 BECHAR (08000), Algeria
gasbaoui_2009@yahoo.com

Abstract

The Next Future Commercialized 4WD Electric Vehicle Future (EV) is designed to minimize the autonomous, the time range of starting and acceleration, in order to improve the vehicle stability and the other dynamic performances for this reason the multi-input multi-output fuzzy logic controller (MIMO-FLC) was presented and implemented in the electrical traction system forming the maximum control process, the advantages of this control structure (MIMO-FLC) is to give more and more safety and stability for the 4WD comparing with the classical fuzzy controller , The main object of this paper is to show the efficiency of the MIMO-FLC applied on four speeds electric vehicles, the 4WD is powered by four induction motors of 15 kilowatts of each one developing an effort of 338 N. m as global torque so this kind of vehicle consist of two front directing wheels and rear propulsion wheels . The MIMO-FLC control technique is simulated in MATLAB SIMULINK environment. The simulation results proves that the MIMO-FLC method decreases the error speeds of the differential electronic at any curves and mainting the vehicle stability at the curved roads when the transient oscillations are decreased and give good dynamical performance for the vehicle using four induction motors for motion ,it's clearly that the proposed control present more robustness comparing with the SISO classical ones which have many more problems during the vehicle driving , the results obtained present satisfactory and the vehicle designer must take into consideration the stability effect for the 4WD vehicle moving in road with different topologies using the MIMO-FLC control.

Keywords: *4WD, MIMO-FLC, SISO-FLC, vehicle control, stability, safety*

1. Introduction

The principal constraints in vehicle design for transportation are the development of a non-polluting high safety and comfortable vehicle. Taking into account these constraints, our interest has been focused on the 4WD electrical vehicle, with independent driving wheel-motor at the front and with classical motors on the rear drive shaft [1, 2, 3, 4]. This configuration is a conceivable solution, the pollution of this vehicle is strongly decreased and electric traction gives the possibility to achieve accurate and quick control of the distribution torque. Torque control can be ensured by the inverter, so this vehicle does not require a mechanical differential gear or gearbox. One of the main issues in the design of this vehicle (without mechanical differential) is to assume the car stability. During normal driving condition, all drive wheel system requires a symmetrical distribution of torque in the both sides. In recent years, due to problems like the energy crisis and environmental pollution, the Electric Vehicle (EV) has been researched and developed more and more extensively. Currently, most EVs are driven by two front wheels or two rear wheels. Considering some efficiency and space restrictions on the vehicle, people have paid more and more attention in

recent years to four-wheel drive vehicles employing the IM in-wheel motor. The researchers assumed that wheel motors were all identical with the same torque constant; neglecting motor dynamics the output torque was simply proportional to the input current with a prescribed torque constant.

DTC_SVM method is an advanced, computation intensive PWM method and possibly the best among all the PWM techniques for variable speed drives application [19]. Because of its superior performance characteristics, it has been finding widespread application in recent years. With a machine load, the load neutral is normally isolated, which causes interaction among the phases. This interaction was not considered before in the PWM discussion. Recently, fuzzy logic control has found many applications in the past decades, which overcomes these drawbacks. Hence, fuzzy logic control has the capability to control nonlinear, uncertain systems even in the case where no mathematical model is available for the controlled system.

The majority of process industries are nonlinear, multi- input multi-output (MIMO) systems. The control of these systems is met with a number of difficulties due to process interactions, dead time and process nonlinearities [7]. The difference between MIMO systems control and Single-Input Single-Output (SISO) systems control is based on an estimation and compensation of the process interaction among each degree of freedom. It is obvious that the difficulty of MIMO systems control is how to overcome the coupling effects among each degree of freedom. To obtain good performance, coupling effect cannot be neglected. Hence SISO system control scheme is not easy to implement on complicated MIMO systems [8, 9]. In addition, the control rules and controller computation will grow exponentially with respect to a number of considered variables. Therefore, intelligent control strategy is gradually drawing attention.

The structure of the work presented in this paper is organized in the following sequence: The principle components of the Electric traction chain with their equations model is set in Section 2. Section 3 shows the development space vector modulation technique based DTC for Electric vehicle motorization. The multi-input multi-output fuzzy logic controller (MIMO-FLC is given in the Section 4. The simulation results are presented in Section 5. Finally, the concluding remarks are given in Section 6.

2. Electric Vehicle Mechanical Load Description

According to Figure 1 the vehicle torque results from many forces such as: the tire forces F_{tire}, the aerodynamic force F_{aero}, the hill climbing force F_{slope} where the total resistive force is equal to F_r [1,2 3],it's given by :

$$F_r = F_{tire} + F_{aero} + F_{slope} \tag{1}$$

The rolling resistance force is defined by:

$$F_{tire} = mgf_r. \tag{2}$$

The aerodynamic resistance torque is defined as follows:

$$F_{aero} = \frac{1}{2}\rho_{air} A_f C_d v^2 \tag{3}$$

The rolling resistance force is usually modeled as:

$$F_{slope} = mg\sin(\beta) \tag{4}$$

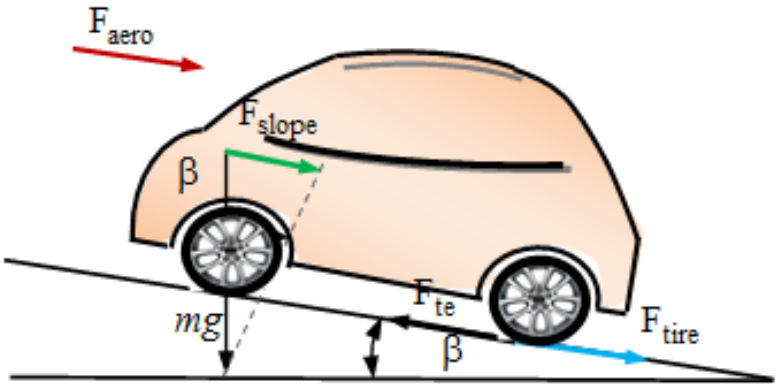

Figure 1. The Forces Acting on a Vehicle Moving Along a Slope

Where is the tire radius, m is the vehicle total mass, is the rolling resistance force constant, the gravity acceleration, is Air density, is the aerodynamic drag coefficient, is the frontal surface area of the vehicle, is the vehicle speed, is the road slope angle.

3. Direct Torque Control Strategy Based Space Vector Modulation (SVM-DTC)

In this technique two proportional integral (PI) type controllers are used instead of hysteresis band regulating the torque and the magnitude of flux as it shown in Figure 2, by generating the voltage command for inverter control. Noting that no decoupling mechanism is required as the flux magnitude and the torque can be regulated easily by the PI controllers. Due to the structure of the inverter, the DC bus voltage is fixed, therefore the speed of voltage space vectors are not controllable, but we can adjust the speed by means of inserting the zero voltage vectors to control the electromagnetic torque generated by the induction motor. The selection of vectors is also changed. It is not based on the region of the flux linkage, but on the error vector between the expected and the estimated flux linkage [13, 14, 15].

The induction motor stator flux can be estimated by:

$$\phi_{ds} = \int_0^t (V_{ds} - R_s i_{ds}) dt \tag{5}$$

$$\phi_{qs} = \int_0^t (V_{qs} - R_s i_{qs}) dt \tag{6}$$

$$|\phi_s| = \sqrt{\phi_{ds}^2 + \phi_{qs}^2} \tag{7}$$

$$\theta_s = \tan^{-1}\left(\frac{\phi_{qs}}{\phi_{ds}}\right) \tag{8}$$

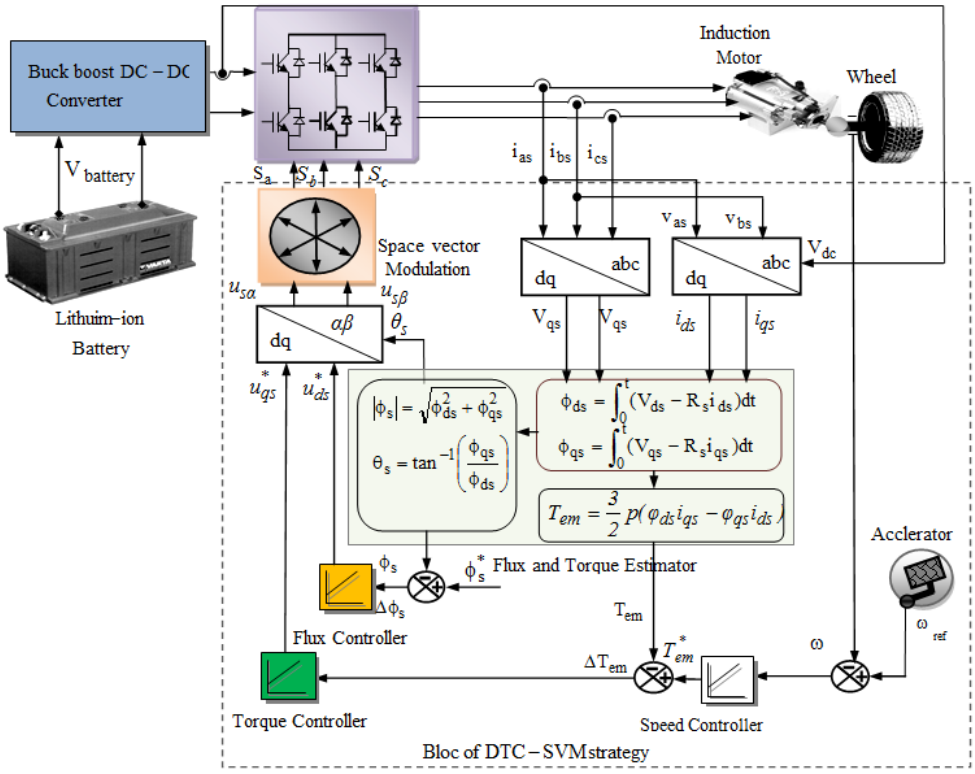

Figure 2. Bloc Diagram for DTC Strategy based Space Vector Modulation

The electromagnetic torque can be given as follow:

$$T_{em} = \frac{3}{2} p(\phi_{ds} i_{qs} - \phi_{qs} i_{ds}) \tag{9}$$

The SVM principle is based on the switching between two adjacent active vectors and two zero vectors during one switching period. It uses the space vector concept to compute the duty cycle of the switches.

4. Multi-Input Multi-Output Fuzzy Controller Structure

Fuzzy set theory has been successfully applied in a number of control applications [8, 12] based on the SISO system point of view without system model consideration. In this paper, the MIMO fuzzy control strategy is used to multi-machines system speed control. The design procedure of the fuzzy control strategy is used to control each degree of freedom of this MIMO system individually. Then, an appropriate coupling fuzzy logic controller (FLC) is designed to compensate for the coupling effects of system dynamics among each degree of freedom.

An ordinary fuzzy controller that usually operates with system output error and error change was chosen as the main controller to control each degree of freedom of the MIMO systems. Here, the input variables of the conventional fuzzy controller for among each degree of freedom of a MIMO system were defined individually as:

$$e_i(k) = \omega_i^*(k) - \omega_i(k) \tag{10}$$

$$\Delta e_i(k) = e_i(k) - e_i(k-1) \tag{11}$$

Where is the position error of the degree, is used for change in error of the degree, is the reference input (Rotation speed reference of the roller i) of the degree and represents the position output of each degree of freedom (real Rotation speed of the roller i) of this MIMO system at the sample. The relationship between the scaling factors are the input and output variables of the FLC.

$$e_{iN} = G_e \times e_i, \Delta e_{iN} = G_{\Delta e} \times \Delta e_i, \Delta u_i = G_{\Delta u} \times \Delta u_{iN} \quad (12)$$

Selection of suitable values for, and are made based on the knowledge about the process to be controlled and sometimes through trial and error to achieve the best possible control performance. This is so because, unlike conventional no fuzzy controllers to date, there is no well-defined method for good setting of scaling factor's for FLC's. The SFs are the significant parameters of FLC because changing the SFs changes the normalized universe of discourse, the domains, and the membership functions of input/output variables of FLC. All membership functions (MFs) for controller inputs (and) and incremental change in controller output ( ) are defined on the common normalized domain (Per Unit) [-1, +1]. We use symmetric triangles (except the two MFs at the extreme ends) with equal base and 50% overlap with neighboring MFs as shown in Figure 3. This is the most natural and unbiased choice for MFs. By way of the above design process, the actual control input voltage for the main fuzzy controller can be written as:

$$u_i(k) = u_i(k-1) + \Delta u_i(k) \quad (13)$$

In (13), is the sampling instant and is the incremental change in controller output, which is determined by the rules of the form (IF-THEN) If is and is Then is. The rule base for computing is a standard one [8, 12, 29] as shown in Table 1.

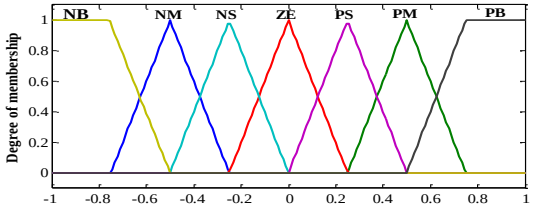

Figure 3. Membership Functions $e_i, \Delta e_i$ and Δu_i

Where:**NB**-Negative Big, **NM**-Negative Medium, **NS** Negative Small, **ZE**-Zero Error, **PS**-Positive Small, **PM**-Positive Medium, **PB**-Positive Big.

Table 1. Rules Base

Δe_{il} / e_i	NB	NM	NS	ZE	PS	PM	PB
NB	NB	NB	NB	NM	NS	NS	ZE
NM	NB	NM	NM	NM	NS	ZE	PS
NS	NB	NM	NS	NS	ZE	PS	PM
ZE	NB	NM	NS	ZE	PS	PM	PB
PS	NM	NS	ZE	PS	PS	PM	PB
PM	NS	ZE	PS	PM	PM	PM	PB
PB	ZE	PS	PS	PM	PB	PB	PB

The fuzzy control rules of the coupling fuzzy controller are similar to the main fuzzy controller. The output of the coupling fuzzy controller is chosen directly as the coupling control input voltage. The main reason is that there is a different coupling effect for each sampling interval and it does not have an accumulating feature. The coupling effect is incorporated into the main fuzzy controller for each step to improve system performance and robustness. Figure 4, illustrates the structure of MIMO fuzzy control scheme. Therefore, the total control input voltage of the MIMO fuzzy controller is represented as:

$$u_i(k) = u_i(k) + U(k)_{i \to l} \quad , \quad i \neq l \tag{12}$$

Where expresses the system control input voltage of the degree of a main fuzzy controller. represents the coupling effect control of the degree relative to the degree of the coupling fuzzy controller.

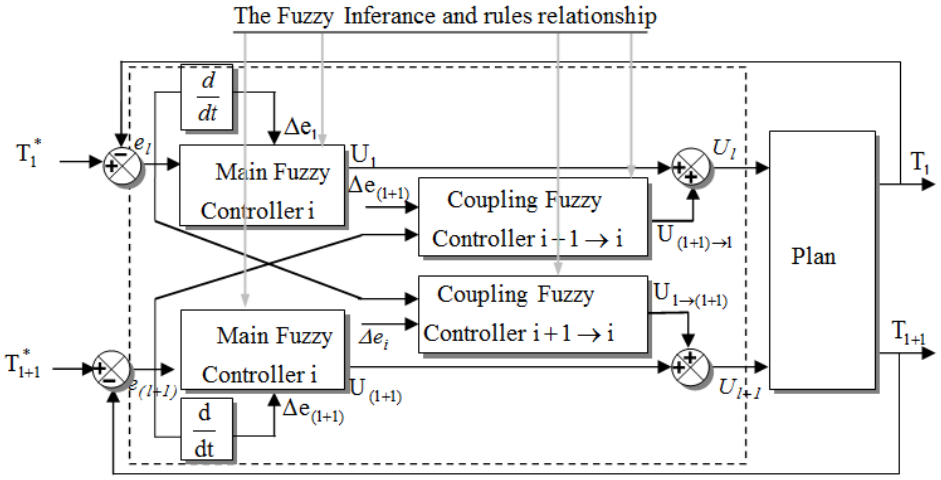

Figure 4. Structure of MIMO Fuzzy Control Scheme

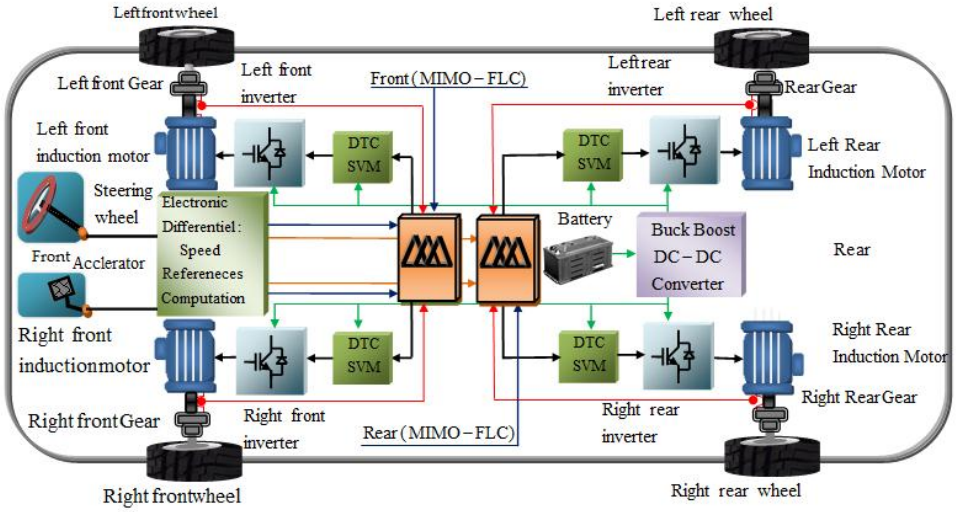

Figure 5. The Driving Wheels System with MIMO-FLC Controller

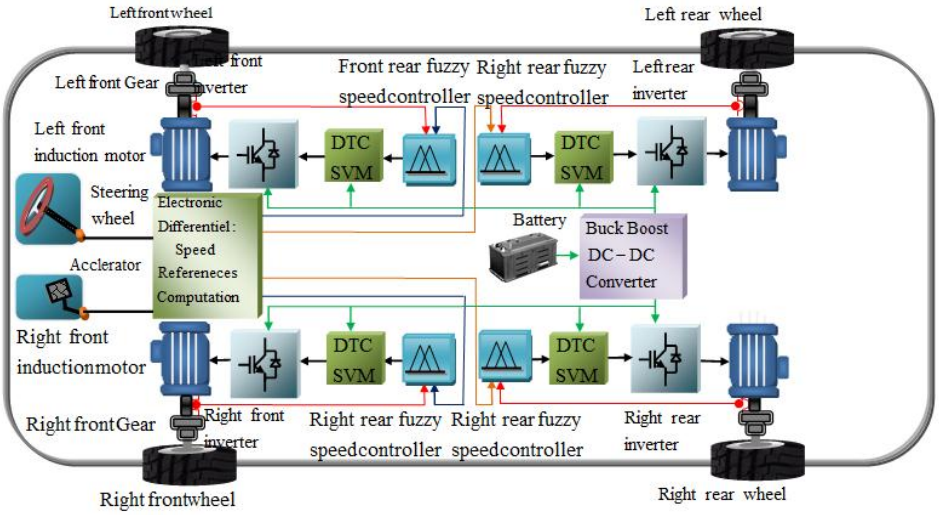

Figure 6. The Driving Wheels System with SISO-FLC Controller

5. Simulation Results

In order to analyze the driving wheel system behavior, Simulations were carried using the model of Figures 5 and 6.The following results were simulated in MATLAB and its divided in two phases .the first one deal with the test of the EV performances controlled with DTC-SVM strategy under several topology variation in the other hand we show the impact of this controller on vehicle power electronics performances. Only the right motor simulations are shown. The assumption that the initialized lithium-ion battery SOC is equal to 70% during trajectories.

The topology studied in this present work consists of four phases: the first one is the beginning phases with a speed of 80 Km/h in straight road topology; the second phases present the sloped road. The third phase is the curved road with the same speed, finally the 4WD moving up the descent road about 10% under 80 Km/h, the detail are shown in Figure 7.

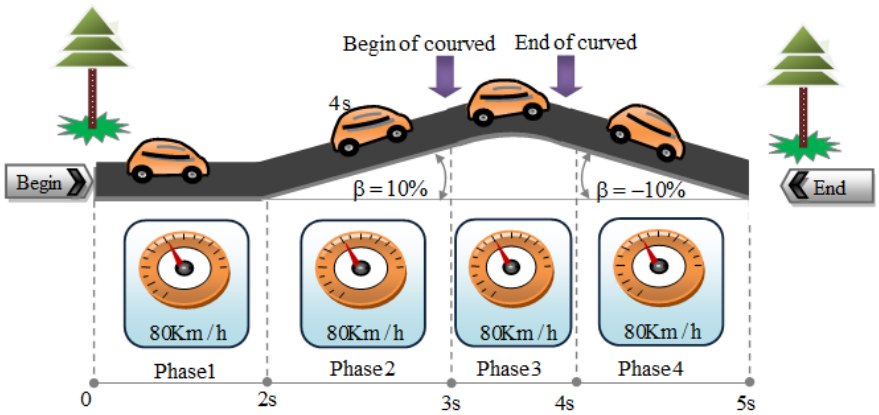

Figure 7. The Chosen Road Topology of Tests

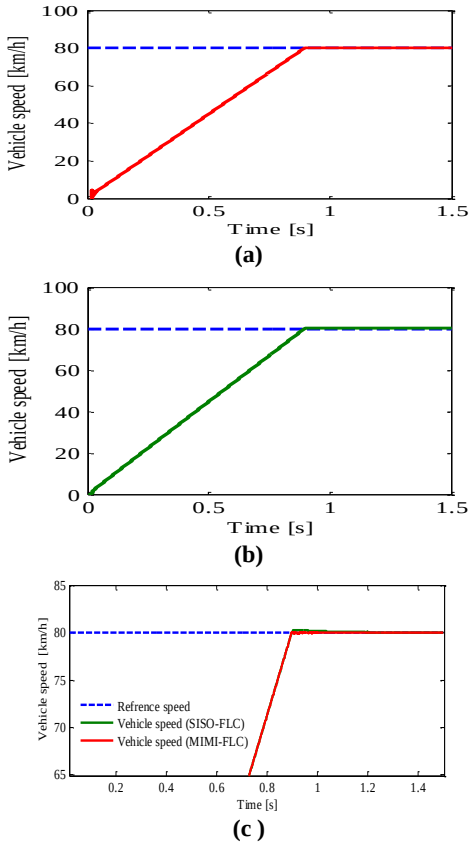

Figure 8(a) Zoomed of the vehicle speed response with (MIMO-FLC) speed controller; (b) Zoomed of the vehicle speed response with (SISO-FLC) Speed controller; (c) Zoomed of vehicle speed for two controller cases

To compare the effect of disturbances on the 4WD electric vehicle speed of two types of control, Figure 8 shows the system response in two cases (MIMO-FLC, and SISO-FLC). We can summarize the vehicle speed results in the following table:

Table 2. Performances of the MIMO-FLC & SISO-FLC in the Speed Loop Response

Results	Overshoot [%]	Rising time [sec]	Steady state [%]
SISO-FLC	0.5600	0.9082	1.0182e+001
MIMO -FLC	0.0141	0.8952	6.8533e+000

According to Figure 9 and Table 2, we can say that the effect of the disturbance is neglected in the case of the MIMO-FLC. It appears clearly that the classical control with SISO-FLC is easy to apply. However the control with MIMO-FLC offer better performances in the rising time control and overshoot. In addition to these dynamic performances, it respects the imposed constraints by the driving system such as the robustness of parameter variations.

A: Multi-input Multi-Output Fuzzy Logic Controller MIMO-FLC for Direct torque control based space vector modulation scheme.

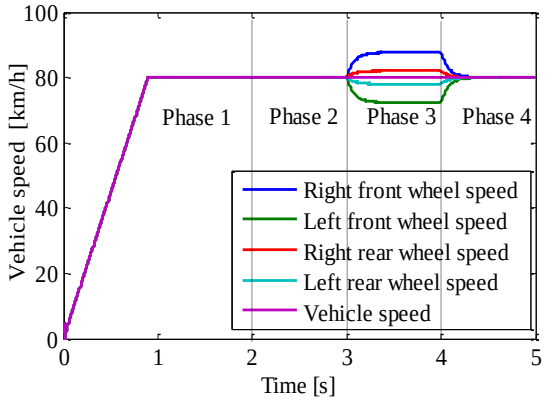

Figure 9. Variation of Vehicle Speeds in Different Phases

Refereed to Figure 9 at time of 2s the vehicle driver or driving in the straight road, this test explains the effect of the slope on the EV. The driving wheels linear speeds stay the same and the road drop does not influence the torque control of each wheel turns the steering wheel. At t = 3 the vehicle driver is driving on a curved road on the right side with a speed of 80 km/h, the assumption is that the four motors are not disturbed. In this case the front and rear driving on a curved road at the right side with a speed of 80 km/h, the assumption is that the four motors are not disturbed. In this case the front and rear driving wheels follow different paths, and they turn in the same direction but with different speeds. The electronic differential acts on the four motor speeds by decreasing the speed of the driving wheel on the right side situated inside the curve, and on the other hand by increasing the wheel motor speed on the external side of the curve. The behaviors of these speeds are given in Figure 8. At t = 4 s the vehicle situated in the second curve but in the left side, the electronic differential computes the novel steering wheels speeds references in order to stabilize the vehicle inside the curve. The battery initial SOC of 70 % is respected. In this case the driving wheels follow the same path with no overshoot and without error which can be justified by the good electronic differential act coupled with DTC performances. The globally distance travelled is 406.50 m in four trajectory phases.

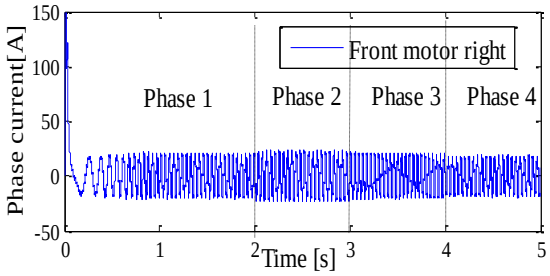

Figure 10. Variation of Phase Current of the Front Motor Right in Different Phases

Figure 10, explains the variation of phase current and electromagnetic torque respectively. In the first step and to reach 80 km/h The EV demand a current of 21.10 A for each motor which explained with electromagnetic torque in 42,26 NM. The second phase explains the effect of the sloped road the electromagnetic torque increase and the current demand undergo double of the current braking phases, The four motor induction develops more and more electromagnetic torque for vanquish the slop They develop approximately 53.97 N.m each one. The linear speeds of the four induction motors stay the same and the road drop does not influence the torque control of each wheel .In the curved road the current and electromagnetic torque demand is computed using the electronic differential process according to the driver decision by means that the speed reference of each wheel is given by the electronic differential computations witch convert the braking angle of the curve on linear speeds. Figure 8 show the electromagnetic torque of the front motor right. The last phase clarifies the effect of the descending slope on the electric vehicle moving on a straight road. The linear speed response is illustrated in Figure 8. The presence of descent causes a great decrease in the phase current of each motor by means that the aerodynamic force became a motor force and the other resistive torques became motor torque the results are listed in Table 3.

Table 3. Values of Phase Current Driving Force of the Right Motor in Different Phases

Phases	1	2	3	4
Current of the front motor right [A]	21.10	23.32	21.10	18.94
Electromagnetic torque of front motor right [N.m]	42.26	53.97	43.37	33.16

According to the formulas (1), (2), (3) and (4) 6, the variety of vehicle torques in different cases as depicted in Figure 11, the vehicle resistive torque was 127.60 N.m in the first case (beginning phase) when the power propulsion system resistive one is 127.60 N.m in sloped road, the driving wheels develop more and more efforts to satisfy the traction chain demand which justify a resistive torque equal to 168.40 N.m. In the third phase. The result proves that the traction chain under acceleration demand develop the double effort comparing with the descent slope case’s by means that the vehicle needs the half of its energy in the deceleration phase's compared with the acceleration one's.

B: Power electronics.

The lithium-ion battery must be able to supply sufficient power to the EV in accelerating and decelerating phase , which means that the peak power of the batteries supply must be greater than or at least equal to the peak power of both the electric motors. The battery must store sufficient energy to maintain their SOC at a reasonable level during driving, the Figure 11 describes the changes in the battery storage power in different speed references.

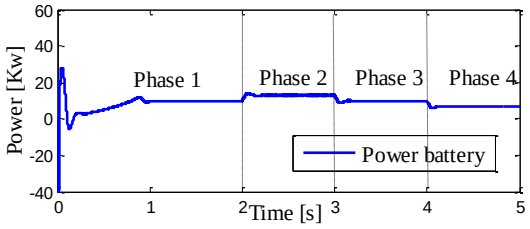

Figure 11. Variation of Lithium-ion Battery Power in Different Phases

It is interesting to describe the power distribution in the electrical traction under several road topology references as it described in Figure 10. The battery provides about 9.86 kWh in the first phase in order to reach the electronic differential reference speed of 80 Km/h. In the second phase (phase 2: sloped phase's) the demanded power battery increase and stagnate at 61.71 % of the global nominal power battery (21 kW). In the third phase the battery produced power equal to 46.90 kW under curved road state. The battery produced power depend only on the electronic differential consign by means the acceleration/deceleration driver state which can be explained by the battery SOC of Figure 11. In this phase the 4WD electric vehicle helps the battery in order to charge the empty battery cells, the four induction motor absorbed the half of the slopped energy.

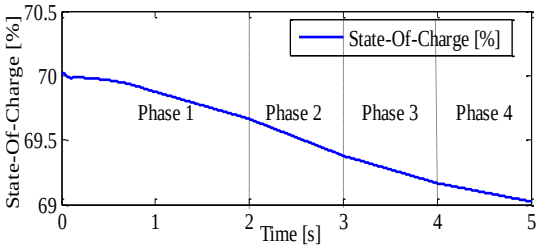

Figure 12. Battery Efficiency versus State-of-charge

Figure 12 explains how SOC in the lithium-ion battery changes during the driving cycle; it seems that the SOC decreases rapidly at acceleration, by means that the SOC range's between 69.02 % to 70% during all cycle's phases from beginning at the end cycles.

At t = 5 s, the battery SOC becomes lower than 69.02 % (it was initialized to 70 % at the beginning of the simula-tion).

Table 4 reflect the variation of SOC in different simulations phases. The relationship between SOC and left time in four phases are defined by the flowing linear fitting formula:

$$SOC[\%] = -0.00049t^6 + 0.0066t^5 - 0.034t^4 + 0.091*t^3 - 0.17t^2 - 0.01t + 70 \quad (14)$$

Moreover we can define the relationship between the sate of charge and the traveled distance in all topologies road.

$$SOC[\%] = 1.8e-008*d_{traveled}^3 - 8.1e-006*d_{traveled}^2 - 0.002*d_{traveled} + 70 \quad (15)$$

Table 4. The Relationship between the Traction Chain Power Electronics Characteristics and the Distance Traveled in Different Phases

	80Km/h Phase1	80Km/h Phase2
$D_{traveled}$ [m]	124.10	80
$SOC_{begin}\% \rightarrow SOC_{end}\%$	$70\% \rightarrow 69.66\%$	$69.66\% \rightarrow 69.38\%$
SOC_{diff} [%]	0.34	0.28
$P_{consumed}$[Kw]	9.85	12.96
Linear Speed	80Km/h Phase3	80Km/h Phase4
Linear Speed	80	80
$D_{traveled}$ [m]	$69.38\% \rightarrow 69.17\%$	$69.17\% \rightarrow 69.02\%$
$SOC_{begin}\% \rightarrow SOC_{end}\%$	0.21	0.15
SOC_{diff} [%]	9.85	6.28
$P_{consumed}$[Kw]		

This power is controlled by the Buck Boost DC-DC converter current and distribute accurately for four phases. The buck boost converter is not only a robust converter which ensures the power voltage transmission but also a good battery recharge in deceleration state that help to perfect the vehicle autonomous with no voltage ripple. The comparative study for two cases performance is shown in Table 5. In this paper we have presented comparative studies between MIMO- FLC and SISO-FLC speed controller. The MIMO-FLC controller method gives a satisfaction results for electric vehicle speed performance.

Table 5. Comparative Study of Second Phases

Parameter and indexes	MIMO-FLC	SISO-FLC
Aerodynamic torque [Nm]	73.30	73.09
Vehicle torque [Nm]	168.40	168.99
Current torque of the front motor right [A]	23.32	23.93
Electromagnetic torque of the front motor right [Nm]	53.97	54.35

6. Conclusion

In this paper, the 4WD electric vehicle speeds are controlled using multi-input multi-output fuzzy logic controller MIMO-FLC. this results has demonstrated that stability , the safety and autonomous of the vehicle using four wheels for motion moving in curved road topologies can be improved using the MIMO-FLC controller, this kind of control have many more advantages such as it robustness and it's rising time response, after the uses of this strategy the vehicle traction system present more and more dynamical performances, the autonomous is developed, the state of charge is decreased and the driving can be facilitate, the electronic differential using this present strategy is acting immediately at any moment according to the real driver decision with no error in vehicle torque and speed estimation of each wheels with no error, the globally linear speeds is perfected with no overshoots which indicate the efficiency of this controller comparing with the SISO-FLC controller. Finally this results present satisfactory and the 4WD designer must take into consideration the MIMO-FLC process to ensure the safety of boths of vehicle and passenger during the driving.

References

[1] J. Wang, Q. Wang, L. Jin and C. Song, "Independent wheel torque control of 4WD electric vehicle for differential drive assisted steering", Mechatronics, vol. 21, **(2011)**, pp. 63–76.
[2] J. Wang, Q. Wang and L. Jin, "Modeling and simulation studies on differential drive assisted steering for EV with four-wheel-independent-drive", In: Proceedings of the 4th IEEE vehicle power and propulsion conference (VPPC2008), Harbin, China, **(2008)** September.
[3] H. Yoichi, T. Yasushi and T. Yoshimasa, "Traction control of electric vehicle: basic experimental results using the test EV "UOT Electric March", IEEE Trans Ind Appl., vol. 34, no. 5, **(1998)**, pp. 1131–8.
[4] F. Wu and T. J. Yeh, "A control strategy for an electrical vehicle using two in-wheel motors and steering mechanism", In: Proceedings of AVEC'08, **(2008)**, pp. 796–801.
[5] Z. Zhu, *et al.*, "Electrical machines and drives for electric, hybrid, and fuel cell vehicles", Proc. IEEE, vol. 95, no. 4, **(2007)**, pp. 764-765.
[6] P. Vas, "Sensorless Vector and Direct Torque Control", Oxford University Press, **(1998)**.
[7] K. Itoh and H. Kubota, "Thrust ripple reduction of linear induction motor with direct torque control", Proceedings of the Eighth International Conference on Electrical Machines and Systems, ICEMS 1, **(2005)**, pp. 655-658.
[8] L. Chen and K. L. Fang, "A Novel Direct Torque Control for Dual-Three-Phase Induction Motor", Conf. Rec. IEEE International Conference on Machine Learning and Cybernetics, **(2003)**, pp. 876-88.
[9] D. S. Zinger, F. Profumo, T. A. Lipo and D. W. Novotny, "A direct field-oriented controller for induction motor drives using tapped stator windings", IEEE Transactions on Power Electronics, vol. 5, no. 4, **(1990)**, pp. 446-453.
[10] A. Schell, H. Peng, D. Tran and E. Stamos, "Modeling and Control Strategy development for Fuel Cell Electric Vehicle", Annual Review in control Elseiver, vol. 29, **(2005)**, pp. 159-168.
[11] A. Haddoun, "Modeling Analysis and neural network control of an EV Electrical Differentiel", Transaction on industriel electronic, vol. 5, no. 6, **(2008)**.
[12] A. Nasri, A. Hazzab, I. K. Bousserhane, S. Hadjeri and P. Sicard, "Two Wheel Speed Robust Sliding Mode Control For Electric Vehicle Drive", Serbian Journal of Electrical Engineering, vol. 5, no. 2, **(2008)**, pp. 199-216.
[13] K. Hartani, "Electronic Differential with Direct Torque Fuzzy Control for Vehicle Propulsion System", Turk J Elec Eng & Comp Sci, vol. 17, no. 1, **(2009)**.
[14] L. T. Lam and R. Lovey, "Developpement of ultra-battery for hybrid-electric vehicle applications", Elservier, power sources, vol. 158, **(2006)**, pp. 1140-1148.
[15] Larminie, "Electric Vehicle Technology Explained", Edited by John Wiley and John Lowry, England, **(2003)**.
[16] A. Haddoun, *et al.*, "Analysis modeling and neural network of an electric vehicle", in Proc IEEE IEMDC, Antalya Turky, **(2007)**, pp. 854-859.
[17] M. Vasudevan and R. Arumugam, "New direct torque control scheme of induction motor for electric vehicles", 5th Asian Control Conference, vol. 2, **(2004)**, pp. 1377 – 1383.

[18] M. E. H. Benbouzid, *et al.*, "Advanced fault-tolerant control of induction motor drives for EV/HEV traction applications From conventional to modern and intelligent control techniques", IEEE Trans. Veh. Technol., vol. 56, no. 2, **(2007)**, pp. 519-528.
[19] A. Gupta and A. M. Khambadkone, "A space vector pwm scheme for multilevel inverters based on two-level space vector pwm", IEEE Transaction on Industrial Electronics, vol. 53, **(2006)**.
[20] T. G. Habetler, F. Profumo, M. Pastorelli and L. Tolbert, "Direct torque control of induction machines using space vector modulation", IEEE Transaction on Industry Applications, vol. 28, no. 5, **(1992)**, pp. 1045-1053.
[21] J. Holtz, "Pulse width modulation for electronic power conversion", Proceedings of the IEEE, vol. 82, **(1994)**, pp. 1194-1214.
[22] K. Zhou, *et al.*, "Relationship between space-vector modulation and three-phase carrier-based PWM a comprehensive analysis", IEEE Trans. Industrial Electronics, vol. 49, no. 1, **(2002)**, pp. 186-195.

Authors

Brahim GASBAOUI received the electrical engineering diploma from the University Ibn-Khaldoun of TIARET (UIT), in 1993 and the MS degree in 2008 from Bechar University University-Algeria.and the Ph.D. degree from the Faculty of the Sciences and the Technology of the Bechar University Currently he is a teacher of electrical engineering at Bechar University. His research interests include power electronics robust control for electric vehicle and propulsion system, power electronics, antilock brake systems, anti-skid control for electric vehicles drive.

Nasri Abdelfatah was born in 1978 at Bechar-Algeria, he's received the electrical engineering diploma from Bechar Center University-Algeria in 2002, and the Magister degree from the University of Sciences and Technology of Oran (USTO), Algeria in 2006. From 2007 until 2011 he get the PHD degree in Electric vehicle propulsion system control. Currently he is an associate professor at Bechar University, his research interest: vehicle energy management, embedded systems energy storage, 4WD Electric vehicle control and design developpement.

Laoufi Abdellah received the state engineer degree in electrical engineering from the University of Sciences and Technology of Oran (USTO), Algeria, the M.Sc. degree from the Electrical Engineering Institute of the University of Djillali Liabes, Algeria, and the Ph.D. degree from the Electrical Engineering Institute of the University of Djillali Liabes. He is currently professor of electrical engineering at Bechar University. His research interests include power electronics, electric drives control, electric vehicle propulsion system control and their applications.

Youssef Mouloudi received the state engineer degree in Electrical Engineering in 2006 from the University of Bechar and the M.S. degree in 2009 from Bechar University, Algeria. He is currently working toward the doctorate degree. His areas of interest are: Facts systems, power filters, applications of power electronics, and stability improvement.